JOURNAL OF MECHANICAL ENGINEERING AND SCIENCES (JMES)
ISSN: 2289-4659 e-ISSN: 2231-8380
VOL. 15, ISSUE 3, 8262 – 8276
DOI: https://doi.org/10.15282/jmes.15.3.2021.05.0649

ORIGINAL ARTICLE

Thermodynamic investigation of intercooling location effect on supercritical CO_2 recompression Brayton cycle

S. Jarungthammachote

Faculty of Engineering at Sriracha, Kasetsart University Sriracha Campus, 199 Sukhumvit Road, TungSukla, Sriracha, Chonburi, 20230, Thailand
Phone: +6638354580

ABSTRACT – In S-CO_2 recompression Brayton cycle, use of intercooling is a way to improve the cycle efficiency. However, it may decrease the efficiency due to increase of heat rejection. In this work, two S-CO_2 recompression Brayton cycles are investigated using the thermodynamic model. The first cycle has intercoolings in a main compression and a recompression process (MCRCIC) and the second cycle has an intercooling in only the recompression process (RCIC). The thermal efficiencies of both cycles are compared with that of S-CO_2 recompression Brayton cycle with intercooling in the main compression process (MCIC). Effects of a split fraction (*SF*) and a ratio of pressure ratio of the recompression (RPR_{RC}) on the thermal efficiencies of MCRCIC and RCIC are also studied. The study results show that the intercooling of recompressor in MCRCIC and RCIC can reduce the compression power. However, it also rejects heat from the cycle and this leads to increasing added heat in the heater. The thermal efficiency of MCRCIC and RCIC are, then, lower than that of the MCIC. For the effects of RPR_{RC} and *SF* to the thermal efficiency of the cycles, in general, when RPR_{RC} increases, the thermal efficiency decreases due to increasing rejected heat. The increase in *SF* causes increasing thermal efficiency of the cycles and the thermal efficiency, then, decrease when *SF* is beyond the optimal value.

ARTICLE HISTORY
Received: 21st Sept 2020
Revised: 30th Mar 2021
Accepted: 16th Aug 2021

KEYWORDS
Supercritical CO_2;
recompression Brayton cycle;
intercooling;
ratio of pressure ratio;
split fraction.

INTRODUCTION

The supercritical carbon dioxide (S-CO_2) Brayton cycle is a promising technology for the power conversion cycle due to high thermal efficiency, simple cycle layout, and compactness of turbomachinery [1] The CO_2 critical point is at 7.3773 MPa and 304.1282 K [2]. Compression of CO_2 at near critical point significantly reduces a power required in a compressor because it has high density and less compressibility. Ahn et al. [1] summarized that for Brayton cycle, S-CO_2 provided a better efficiency than air. They also pointed out that S-CO_2 Brayton cycle technology could be used with nuclear, waste heat and renewable heat sources.

Many researchers have studied the performances of different S-CO_2 Brayton cycle layouts and the operating parameters affecting these cycle performances. Crespi et al. [3] reviewed different S-CO_2 Brayton cycle layouts for power generation. The cycles were separated into two main categories that were stand-alone cycles and combined cycles. Strengths and weaknesses of the cycles were presented and discussed. Luu et al. [4] conducted a comprehensive study of different S-CO_2 cycle layouts integrated with a concentrated solar thermal plant. Cheang et al. [5] analyzed different S-CO_2 power cycle layouts and compared them to a steam Rankine cycle. In their analysis, it was found that the recompression cycle was the most efficient. A thermodynamic comparison of five S-CO_2 Brayton cycles integrated with a solar power tower was conducted by Al-Sulaiman and Atif [6]. Their study result demonstrated that the highest thermal efficiency was achieved using the recompression Brayton cycle. Di Maio et al. [7] compared a simple S-CO_2 Brayton cycle with the recompression Brayton cycle. The result showed that the efficiency of S-CO_2 recompression Brayton cycle was always above 40% and the recompression Brayton cycle was more efficient than the simple Brayton cycle.

The recompression Brayton cycle was interested by many researchers, because it has high efficiency with a little modification from the simple cycle. Dyreby [8] proposed a mathematical model to analyze the design and off-design performances of S-CO_2 recompression Brayton cycles. Some operating cycle parameters, such as compressor inlet temperature and pressure of recompression Brayton cycle, were investigated to maximize the thermal efficiency. The sensitivity analysis of the recompression Brayton cycle and the partial cooling cycle was done by Novales et al. [9]. From the analysis, the recompression Brayton cycle has a better thermal efficiency and its efficiency was considerably more sensitive regarding a turbomachinery isentropic efficiency and a recuperator efficiency as compared to the partial cooling cycle. The S-CO_2 recompression Brayton cycle was simulated by Saeed et al. [10]. More realistic models for the turbomachinery and the heat exchanger were developed. Recompression S-CO_2 Brayton cycle for use of high temperature heat source, such as the concentrated solar power application, was comprehensively investigated in [11, 12]. Sarkar and Bhattacharyya [13] analyzed the effect of operating parameters on the S-CO_2 recompression Brayton cycle performance with the fixed turbomachinery isentropic efficiency. They showed that the optimal flow split ratio for the recompression Brayton cycle was obtained when the heat capacity ratios of both streams in the low temperature recuperator were similar.

*CORRESPONDING AUTHOR | S. Jarungthammachote | ✉ sompop.j@ku.th

An intercooling process applied in the recompression Brayton cycle provided a clear advantage to the cycle efficiency. Ma et al. [14] investigated the influence of main compression intercooling (MCIC) on the thermal efficiency of the recompression Brayton cycle. The result of their study pointed out that 2.65% efficiency improvement could be achieved by using MCIC. Ruiz-Casanova et al. [15] conducted the thermodynamic analysis of four different S-CO_2 Brayton cycles for low-grade geothermal heat source application. Based on their study conditions, the intercooling recuperated Brayton cycle could achieve the highest electric power output, energy and exergy efficiencies. Yang et al. [16] investigated the performance of four S-CO_2 Brayton cycles including a simple recuperative cycle, reheating cycle, recompression cycle, and intercooling cycle and the cycles were compared under part-load conditions. They found that the integration of intercooling process could improve the cycle efficiency only when the power load exceeds around 60%. Wang et al. [17] compared the performances of different S-CO_2 Brayton cycle layouts. The performance analysis showed that all S-CO_2 Brayton cycles provided high efficiencies. The intercooling could increase the efficiency for high compressor inlet temperatures.

From the literature review, the S-CO_2 recompression Brayton cycle has high thermal efficiency. Moreover, the integration of recompression Brayton cycle and intercooling process in main compression can improve the cycle efficiency. Wang et al. [18] have proposed the two-stage recompression S-CO_2 Brayton cycle, in which the intercooling processes were deployed in main compression and recompression processes. The reheating process was also applied in the two-stage recompression cycle to obtain an advantage from high-temperature solar thermal energy. The thermodynamic analysis of the proposed cycle was conducted and the effect of split ratio (SR) on the cycle efficiency was investigated. The solar-to-electric efficiency and the cost of electricity were focused. The analysis results showed that, at the design point, the optimal SR was 0.55 and the solar-to-energy efficiency was 27.14%.

As found in the above literature that many researchers have investigated different S-CO_2 Brayton cycles. Recently, two-stage recompression cycle has been proposed. However, there are some interesting issues that have not been studied yet. The analysis, presenting the advantage of the additional intercooling or employing intercooling in the recompression, has not been found in the literature review. As well known that, the intercooling can reduce the compression work. Additional intercooling for recompression, however, increases the rejected heat from the cycle. There is a trade-off between reducing recompression work and increasing heat rejection from the cycle and both have effect on the cycle efficiency. Therefore, the objective of this work is to investigate the S-CO_2 recompression Brayton cycle with different locations of the intercooling. The first cycle is the two-stage S-CO_2 recompression Brayton cycle in which two intercoolings are applied in the main compression and recompression processes. This cycle is called MCRCIC. For the second cycle layout, the intercooling is used in only the recompression process and it is referred to as RCIC. The S-CO_2 recompression Brayton cycle with the intercooling in the main compression (MCIC) is considered as a base cycle for benchmarking. The cycle investigations are done based on the thermodynamic model and the effects of a split fraction (SF) and a ratio of pressure ratio in the recompression (RPR_{RC}) on the thermal efficiency of MCRCIC and RCIC are also studied. The thermal efficiencies of the two modified cycles are compared with that of MCIC to show the advantage and disadvantage of the intercooling(s) employed in the cycles.

METHODS

Description of Investigated Cycle Layouts

The layout of S-CO_2 recompression Brayton cycle with the main compression intercooling or MCIC is shown in Figure 1(a). There are twelve main states in this cycle. At a hot side outlet of a low temperature recuperator (LTR), S-CO_2 is split into two streams (state 11). The first stream rejects heat in a precooler and introduced into the main compressor (MC) at state 1 and compressed to high pressure (state 4) with intercooling. It is, then, preheated in the LTR. The second stream is compressed by the recompressor (RC) and mixed with the first stream exiting from the LTR (state 5). The mixed stream is heated in a high temperature recuperator (HTR) and the additional heat is supplied to the stream in the heater to reach the cycle maximum temperature (state 8) before it enters the turbine to generate the power output. The S-CO_2 is expanded to state 9, however, its temperature is still high. This hot stream passes through the HTR and LTR for heat recovery.

Figure 1(b) presents the configuration of the S-CO_2 recompression Brayton cycle called MCRCIC and Figure 1(c) describes the S-CO_2 recompression Brayton cycle called RCIC. For MCRCIC, it is quite similar to the MCIC but there is the additional intercooler in the recompression process. In RCIC, the intercooler is used in only the recompression, instead of the main compression. The total number of states in RCIC is twelve, equal to that in MCIC. However, the same state number may define different states in RCIC, compared to the states in MCIC.

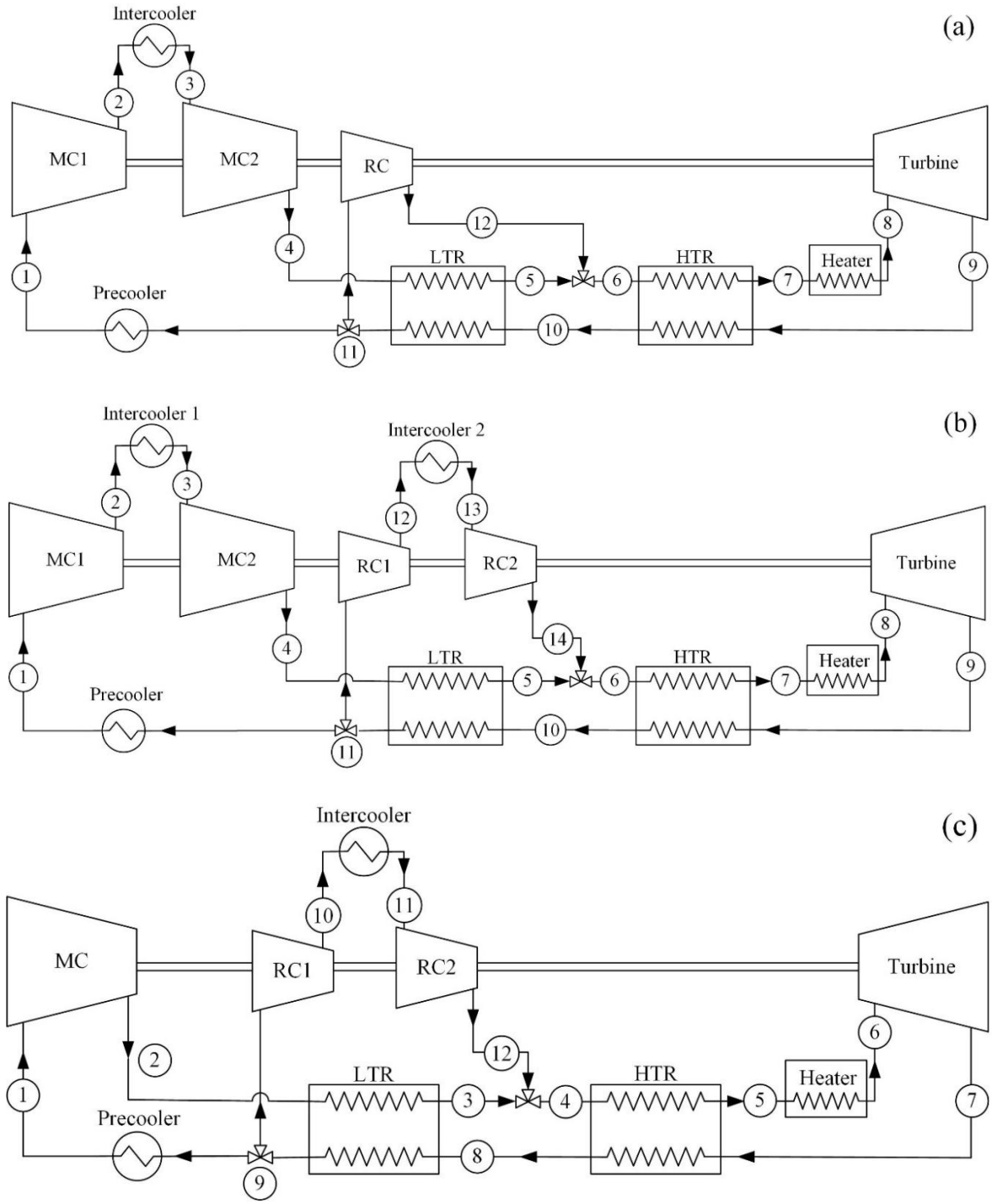

Figure 1. Layout of S-CO_2 recompression Brayton cycle:, (a) with the main compression intercooling (MCIC), (b) with the main compression and recompression intercoolings (MCRCIC) and (c) with the recompression intercooling (RCIC)

Thermodynamic Modelling

The model described here is mainly based on MCIC layout. However, some equations are added or modified to match with MCRCIC and RCIC layouts. The models of the S-CO_2 recompression Brayton cycles are mainly based on the energy balance in each component. The following assumptions are applied in the model development.

1. The heat loss and pressure drop are neglected to consider in the pipe lines.
2. Kinetic and potential energies in each component are neglected.
3. The compressors and turbine are the adiabatic components operated with constant isentropic efficiencies.
4. All components are analyzed in steady state.
5. Pressure drop in intercoolers and recuperators are neglected.

The compression process in the main compressor is divided into two stages with intercooling. For the first compression stage, the inlet pressure and temperature are known as P_1 and T_1, respectively. When the total pressure ratio and the isentropic efficiency of the main compressor are defined as $PR_{MC} = P_4 / P_1$ and $\eta_{isen,MC}$, respectively, the outlet states of the first and second compression stage can be calculated as shown in Eqs. (1) to (4).

$$P_2 = P_1(PR_{MC})^{RPR_{MC}} \tag{1}$$

$$h_2 = h_1 + (h_{2,s} - h_1) / \eta_{isen,MC} \tag{2}$$

$$P_4 = P_3(PR_{MC})^{1-RPR_{MC}} \tag{3}$$

$$h_4 = h_3 + (h_{4,s} - h_3) / \eta_{isen,MC} \tag{4}$$

where the subscripts s and MC represent the isentropic process and the main compression process, respectively. RPR represents the ratio of pressure ratio and RPR_{MC} is defined in Eq. (5) [14].

$$RPR_{MC} = \left[\ln(P_2 / P_1)\right] / \left[\ln(PR_{MC})\right] \tag{5}$$

If the split fraction, SF, is defined as the ratio of mass flow rate through the main compressor to the total mass flow rate $\left(SF = \dot{m}_{MC} / \dot{m}_{tot}\right)$, a total power consumption of the main compressor can be found in Eq. (6).

$$\dot{W}_{MC} = \dot{m}_{tot} \times SF\left[\left(h_2 - h_1\right) + \left(h_4 - h_3\right)\right] \tag{6}$$

For the intercooler in the main compression, the temperature at exit state is assumed to be equal to the temperature at inlet state of the main compressor and no pressure drop is considered. Thus, $T_3 = T_1$ and $P_3 = P_2$.

The outlet state of turbine can be found by P_9, which is the minimum pressure of the cycle, and h_9. To find the enthalpy of the outlet state of turbine $\left(h_9\right)$, the isentropic efficiency of the turbine, $\eta_{isen,T}$, must be primarily defined and Eq. (7) is used.

$$h_9 = h_8 + (h_{9,s} - h_8) / \eta_{isen,T} \tag{7}$$

A power generated from the turbine can be calculated using Eq. (8).

$$\dot{W}_T = \dot{m}_{tot}\left(h_8 - h_9\right) \tag{8}$$

To find the outlet temperature of the hot stream in HTR $\left(T_{10}\right)$, the definition of heat exchanger effectiveness is applied.

$$\varepsilon_{HTR} = \left(T_9 - T_{10}\right) / \left(T_9 - T_6\right) \tag{9}$$

The outlet state of the cold stream can be specified by $P_7 = P_{max}$ and h_7 which can be obtained using the energy balance and the conservation of mass equations. It is finally found that:

$$h_7 = h_6 + h_9 - h_{10} \tag{10}$$

In LTR, the mass flow rate of the hot stream and cold stream are different. Then, the minimum heat capacity is uncertain. Rao et al. [19] suggested to use the enthalpy efficiency instead of the traditional effectiveness for the recuperator modeling. Novales et al. [9] also defined the effectiveness of the recuperator in terms of the enthalpy. However, the enthalpy efficiency and the traditional effectiveness are quite similar. In this study, the effectiveness of LTR is calculated based on the enthalpy to avoid the iterative procedure for finding the average specific heats of the hot stream and cold stream. The effectiveness of LTR is defined as presented in Eq. (11).

$$\varepsilon_{LTR} = \dot{m}_{tot}(h_{10} - h_{11}) / \dot{Q}_{\max} \tag{11}$$

where

$$\dot{Q}_{\max} = \min\left\{\dot{m}_{tot} SF\left(h(T_{10}, P_{\max}) - h_4\right),\ \dot{m}_{tot}\left(h_{10} - h(T_4, P_{\min})\right)\right\} \tag{12}$$

Using Eqs (11) and (12), the hot stream leaving state (state 11) can be found $\left(P_{11} = P_{max}, h_{11}\right)$. The energy balance is performed to find the cold stream leaving state $\left(P_5 = P_{max}, h_5\right)$ and the enthalpy at state 5 can be obtained using Eq. (13).

$$h_5 = \left[\left(h_{10} - h_{11}\right) / SF\right] + h_4 \tag{13}$$

At the recompression process, the outlet state can be found by the same way as shown in Eq. (2) with $P_{12} = P_{max}$. However, in the case of MCRCIC, the same equations as shown in Eqs. (1) to (4) are applied but the states and compressor parameters must be changed following the parameters and states in the recompression processes of MCRCIC as expressed in Eqs. (14) to (18).

$$P_{12} = P_{11}(PR_{RC})^{RPR_{RC}} \tag{14}$$

$$h_{12} = h_{11} + \left(h_{12,s} - h_{11}\right) / \eta_{isen,RC} \tag{15}$$

$$P_{14} = P_{13}(PR_{RC})^{1-RPR_{RC}} \tag{16}$$

$$h_{14} = h_{13} + \left(h_{14,s} - h_{13}\right) / \eta_{isen,RC} \tag{17}$$

$$\dot{W}_{RC} = \dot{m}_{tot} \times (1 - SF)\left[\left(h_{12} - h_{11}\right) + \left(h_{14} - h_{13}\right)\right] \tag{18}$$

where the subscript RC represents the recompression process.

For mixing between the cold stream leaving from LTR (state 5) and the outlet state of recompression process (state 12), the energy balance is applied to find state 6 $\left(P_6 = P_{max}, h_6\right)$. The enthalpy at state 6 can be calculated using Eq. (19).

$$h_6 = (SF)h_5 + (1 - SF)h_{12} \tag{19}$$

A heat rate supplied to the cycle in the heater and the thermal efficiency of the cycle can be calculated, respectively, by using Eqs. (20) and (21).

$$\dot{Q}_{add} = \dot{m}_{tot}\left(h_8 - h_7\right) \tag{20}$$

$$\eta_{th} = \left(\dot{W}_T - \dot{W}_{MC} - \dot{W}_{RC}\right) / \dot{Q}_{add} = 1 - \sum \dot{Q}_{rej} / \dot{Q}_{add} \tag{21}$$

where $\sum \dot{Q}_{rej}$ is the sum of heat rate rejected in the intercoolers and precooler.

The simulations of MCIC and MCRCIC are described in Figure 2. The simulation starts with specifying the parameters of components and operating conditions. For MCIC modeling, the value of RPR_{RC} in Eqs. (14) and (16) is zero. In Eq. (14), it leads to $P_{12} = P_{11}$ or there is no recompression process and in Eq. (16), it shows $P_{14} = P_{13}(PR_{RC})$ which means that there is one recompression stage with the compression of PR_{RC}. Only one recompression stage means no intercooling and this is the characteristic of MCIC. For RCIC, it has only one compression stage in the main compressor and only one compression stage implies no intercooling in this compression. Therefore, RPR_{MC} in Eqs.(1) and (3) must be zero. Eq. (1) shows on compression in this stage $\left(P_2 = P_1\right)$ and Eq. (3) indicates that there is only one compression process in the main compressor $\left(P_4 = P_3(PR_{MC})\right)$ with the compression ratio of RPR_{MC}. The calculations in the main compressor and turbine are firstly conducted. The temperature at state 6 is initially assumed. The simulations of HTR, heater and LTR are performed. Then, the recompressor is simulated and its outlet state is used to find a new state 6 in mixing process. The new temperature of state 6 is compared with the assumed temperature of state 6. If the temperature difference is more than 0.01K, the temperature of state 6 will be updated and the iterative calculations are conducted only the components confined by the dash line presented in Figure 2 until the criterion is met. The equations used to simulate the processes in MCIC and MCRCIC can be applied in RCIC, but the state numbers defined in the equations are changed to match with the state numbers in RCIC.

Thermodynamic Properties of CO_2

The thermodynamic properties of CO_2 used in this work are calculated using the equation of state developed by Span and Wanger (SW EoS) [2]. The SW EoS is widely used in many researches involving CO_2 because it can provide high accurate result for a wide range of pressure and temperature. Baltadjiev et al. [20] showed that SW EoS has recently gained popularity due to emerging new applications of supercritical CO_2. In SW EoS, the thermodynamic properties are described in terms of the Helmholtz energy which is a function of reduced density (ρ/ρ_c) and inverse of reduced temperature (T_c/T). The critical density, ρ_c, and the critical temperature, T_c, are 467.6 kg/m^3 and 304.1282 K, respectively [2]. To find CO_2 properties at a specific thermodynamic state, the temperature and density are essentially known. However, in a power cycle, temperature and pressure or pressure and enthalpy of working fluid are known instead of temperature and density. A numerical technique, called secant method, is performed to find the temperature and density from knowing properties.

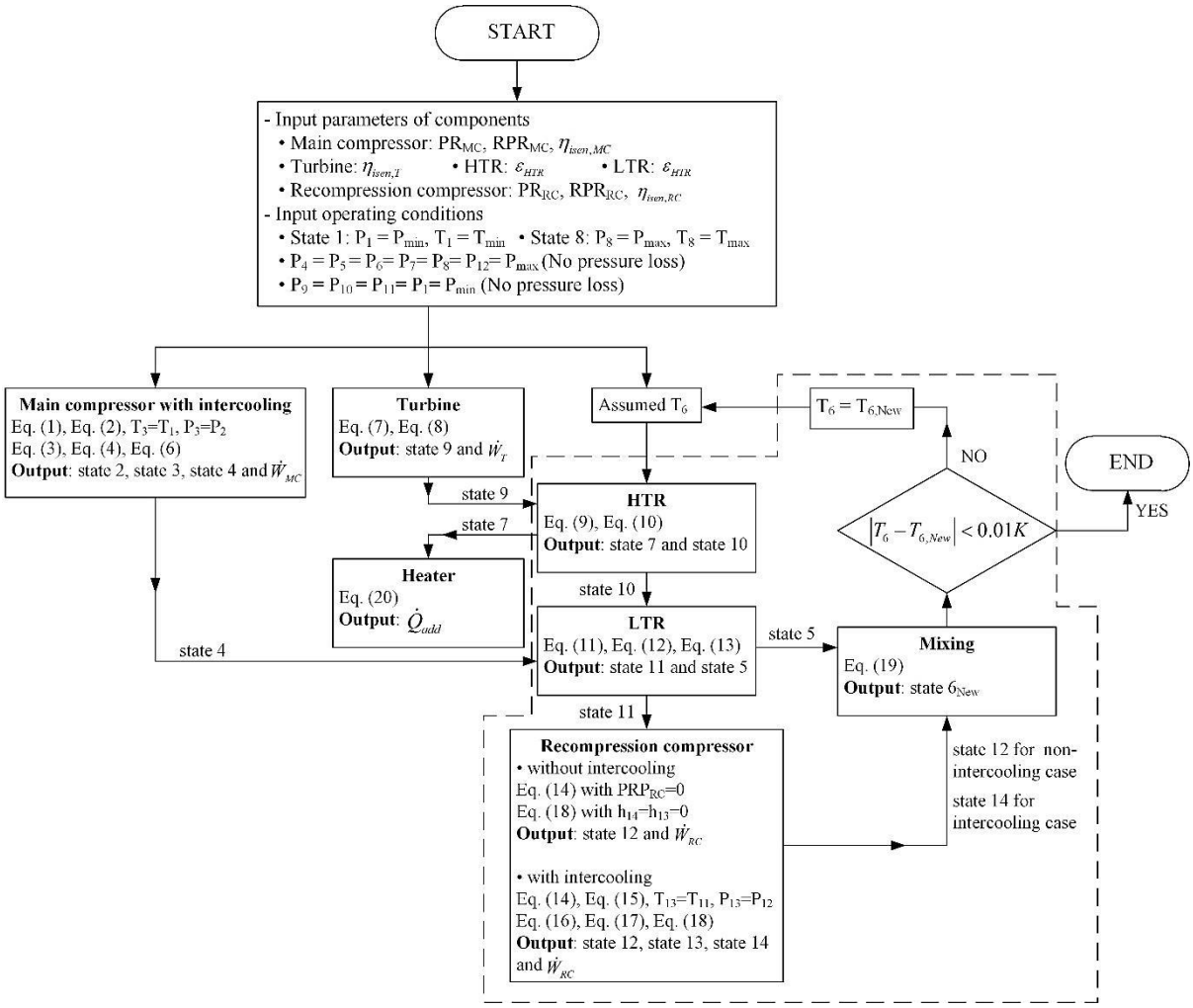

Figure 2. Calculation procedure for the S-CO_2 recompression Brayton cycles

Model Validation

The model validation is divided into two parts. The first one is the validation of thermodynamic properties of CO_2 and the second is the validation of the S-CO_2 recompression cycle modelling. The CO_2 properties consisting of density, enthalpy, and entropy, at different pressures and temperatures are computed using developed computer code. These properties are validated with the properties shown in Span and Wanger's work [2]. Moreover, the reference state values for enthalpy and entropy of CO_2 are adjusted and the calculated properties, i.e. the density, enthalpy, and entropy, are validated with the data from NIST chemistry WebBook [21]. To validate the developed thermodynamic model of the S-CO_2 recompression cycle, the data from three sources, Ma et al. [14], Halimi and Shu [22] and Moisseytsev and Sienicki [23] are used. The simulation results S-CO_2 recompression Brayton cycle with intercooling in main compression ($RPR_{RC} = 0$) are compared with the results available in Ma et al.'s work [14] and the comparison results are shown in Table 1. In Table 2, the validation of simple S-CO_2 recompression cycle is presented. The simulation results from the

model developed in this study are compared with the results from the model developed in Halimi and Shu [22] and Moisseytsev and Sienicki [23].

It should be firstly mentioned here that the state points in Table 1 are referred to the state points defined in Ma et al.'s work [14], they are not the states in Fig 1. From Table 1, it can be observed that the pressure and temperature in each state, the turbine work, the main compression and recompression works and the thermal efficiency, simulated from the present model show the agreement with the results presented in Ma et al.'s work [14].

For the validation shown in Table 2, it is found that the temperatures, enthalpies, and entropies obtained from this study and the references are consistent. For the pressure values in parentheses, they are calculated in this study based on the assumption of no pressure loss, except the pressure at the turbine exit state (state 7). For this validation, the pressure at state 7 in the developed model is defined to be equal to the pressure shown in the published references.

Table 1. Comparison between the simulation results and the results from Ma et al. [14]

State point	Present study		Ma et al.		Performance Parameter	Present study	Ma et al.
	T (K)	P (kPa)	T (K)	P (kPa)			
1	308.15	6250	308.15	6250	SF	64.7 %	64.7 %
2	328.55	8072.59	328.53	8072.59	$\dot{W}_T / \dot{m}_{tot}$	169.36 kJ/kg	169.36 kJ/kg
3	308.15	8072.59	308.15	8072.59	$\dot{W}_{MC} / \dot{m}_{tot}$	22.36 kJ/kg	22.31 kJ/kg
4	347.98	20000	347.96	20000	$\dot{W}_{RC} / \dot{m}_{tot}$	29.06 kJ/kg	29.10 kJ/kg
5	471.08	20000	469.35	20000	$\dot{Q}_{add} / \dot{m}_{tot}$	235.04 kJ/kg	N/A
6	733.95	20000	733.46	20000	η_{th}	50.18 %	50.05 %
7	923.15	20000	923.15	20000			
8	776.56	6250	776.56	6250			
9	486.35	6250	484.71	6250			
10	354.09	6250	354.80	6250			

Table 2. Comparison between the simulation results and the results from Halimi and Shu [22] (H&S) and Moisseytsev and Sienicki [23] (M&S)

State point	Pressure (MPa)	Temperature (K)			Enthalpy (kJ/kg)			Entropy (J/kg·K)		
		Present study	H&S	M&S	Present study	H&S	M&S	Present study	H&S	M&S
1	7.40 (7.40)	304.4	304	304	360.0	360	360	1524.8	1525	1525
2	20.00 (20.00)	357.8	358	358	388.4	388	389	1531.5	1531	1534
3	19.98 (20.00)	462.1	462	465	582.3	582	587	2013.4	2012	2024
4	19.98 (20.00)	460.1	459	462	578.7	578	583	2005.8	2005	2015
5	19.93 (20.00)	670.3	670	672	847.0	847	849	2488.4	2489	2492
6	19.88 (20.00)	814.1	814	814	1024.0	1024	1024	2727.5	2729	2729
7	7.71 (7.71)	700.3	701	700	899.4	900	899	2745.2	2746	2745
8	7.58 (7.40)	464.1	465	466	631.7	632	634	2287.3	2283	2287
9	7.41 (7.40)	359.1	359	359	505.7	506	506	1978.3	1979	1980
10	19.98 (20.00)	455.1	455	457	572.2	572	575	1991.5	1992	1998

RESULTS AND DISCUSSION

Comparison of The Recompression Brayton Cycles

The simulations of the MCIC, MCRCIC, and RCIC cycles are conducted based on a specific reference condition. The performance parameters, such as the thermal efficiency and the cycle operation states, are compared and discussed in this section. The cycle operating parameters used in the simulation are presented in Table 3. For MCIC, SF employed in the simulation is 0.645 which is the optimal SF for MCIC leading to the maximum thermal efficiency. To require the same power for the main compression process, $SF = 0.645$ is also applied to simulate the MCRCIC. Setting the same main compression power required, it can display the effect of the additional intercooling in recompression process to the cycle operation states and the performance parameters. However, in the comparison of thermal efficiency, setting the same value of SF in the comparison may cause the argument that MCRCIC may have higher thermal efficiency than that in the simulation result and its thermal efficiency may be higher than that of MCIC, if MCRCIC is operated at the optimal SF and optimal RPR_{RC}. Therefore, this argument will be discussed later. For RCIC, there is no intercooling in the main compression. The optimal SF is found as 0.662. The simulation of three S-CO_2 recompression Brayton cycles are conducted and the performance parameters obtained from the simulation are shown in Table 4.

Table 3. Cycle operating parameters used in the comparison

Parameter	MCIC	MCRCIC	RCIC
SF	0.645[a]	0.645	0.662[a]
RPR_{MC}	0.25	0.25	0.00
RPR_{RC}	0.00	0.25	0.25
$\eta_{isen,MC}$	0.89	0.89	0.89
$\eta_{isen,RC}$	0.89	0.89	0.89
$\eta_{isen,T}$	0.90	0.90	0.90
ε_{HTR}	0.93	0.93	0.93
ε_{LTR}	0.93	0.93	0.93
P_{max} (MPa)	20.00	20.00	20.00
T_{max} (K)	873.50	873.50	873.50
P_{min} (MPa)	7.40	7.40	7.40
T_{min} (K)	304.40	304.40	304.40

[a] optimal value

In Table 4, the power generated from the turbine and power consumption in main compression process of MCIC and MCRCIC cycles are the same. Nevertheless, the recompressor in MCRCIC demands obviously lower power than the power for recompressor in MCIC because of the intercooling in the recompression process of MCRCIC. As found in Table 4, the intercooling process in the recompression compressor not only reduces the required power but also increases heat input in the heater $(\dot{Q}_{add})$ to reach the maximum temperature of working fluid before flowing into the turbine. This finally leads to lower thermal efficiency of MCRCIC compared to the thermal efficiency of MCIC. For RCIC compared to MCIC, it gives the same power output from turbine. However, the main compression process in RCIC needs more power input due to operating with higher SF value and without intercooling. Moreover, the recompression power required in RCIC is obviously higher than that of MCIC and MCRCIC even through it has intercooling process in recompression process. This is due to fact that, the working fluid passing the main compressor is raised its temperature. It, then, flows into LTR as the cold stream. Therefore, the heat rate transferring from the hot stream to the clod stream is small due to small temperature difference. The temperature of the hot stream is still high. Thus, when the hot stream flows into the recompressor, it demands more power to compress. However, RCIC requires slightly lower heat input than that required in MCIC. This results the thermal efficiency of RCIC marginally lower than the thermal efficiency of MCIC.

Table 4. Cycle performance parameters obtained from simulations

Parameter	MCIC	MCRCIC	RCIC
$\dot{W}_T$ (kW)	138.392	138.392	138.392
$\dot{W}_{MC}$ (kW)	13.604	13.604	19.361
$\dot{W}_{RC}$ (kW)	18.774	14.832	21.585
$\dot{Q}_{add}$ (kW)	222.814	244.588	210.913
η_{th} (%)	47.580	44.956	46.202

In order to make the above discussion be more clear, T-s diagrams of MCRCIC and RCIC compared with MCIC are illustrated in Figures 3(a) and 3(b), respectively. In Figure 3(a), the numbers in parentheses indicate the state points of MCRCIC defined in Figure 1(b) and the numbers without parentheses show the state points of MCIC presented in Figure 1(a). Based on the operating parameters defined in Table 3, states 1 to 4, 8 and 9 of MCIC and MCRCIC are identical. After recompression process, working fluid in MCRCIC (state (14)) has lower temperature than that in MCIC (state (12)) even the recompressor inlet state of both cycles are almost identical. This is because the intercooling process in the recompression process of MCRCIC rejects heat from the working fluid. Then, the working fluid flows into HTR, known as the cold stream of HTR, and it gains the energy from the hot stream. The temperature of cold stream outlet state of HTR in MCRCIC (state (7)) is clearly lower than that in MCIC (state 7). Consequently, it demands more energy in the heater to raise its temperature to reach the state 8. However, the reduction of recompression power of MCRCIC gains less benefit than the increasing added heat in the heater. This results in that the efficiency of MCRCIC is lower than the efficiency of MCIC.

In Figure 3(b), T-s diagrams of RCIC and MCIC are comparatively presented. The state points of RCIC indicated by the numbers in braces. It is clearly seen that the recompression inlet state (state{9}) has higher temperature when it is compared with that of MCIC (state 11). As well known that the power required for gas compression is dependent on the inlet temperature, higher inlet temperature needs higher power for compression. Even there is the intercooling in the recompression process, the second recompression stage also lifts the temperature up. It, then, mixes with the cold stream of LTR and flows into HTR as the cold stream of HTR at state{4}. Comparing to MCIC, the cold stream inlet temperature of RCIC has clearly higher temperature (state 6 and state {4} in Figure 3(b)). As the cold stream of HTR has high temperature, the amount of heat rate transferring from the hot stream to the cold stream is, then, small. The hot stream finally still has high temperature when it leaves the LTR (state{9}). For the cold stream outlet state of HTR (state {5}), it has slightly higher temperature compared to the same state in MCIC (state 7). Thus, it expects lower heat supplied in the heater to reach the maximum cycle temperature at state {6} (see $\dot{Q}_{add}$ in Table 4).

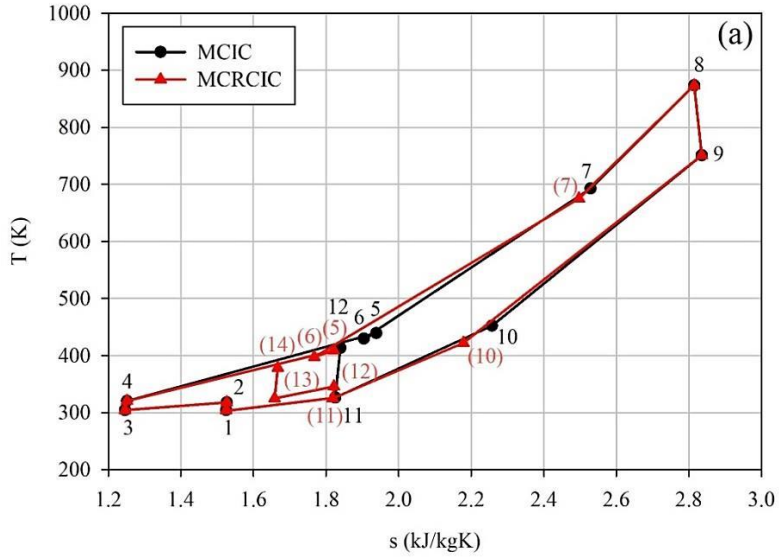

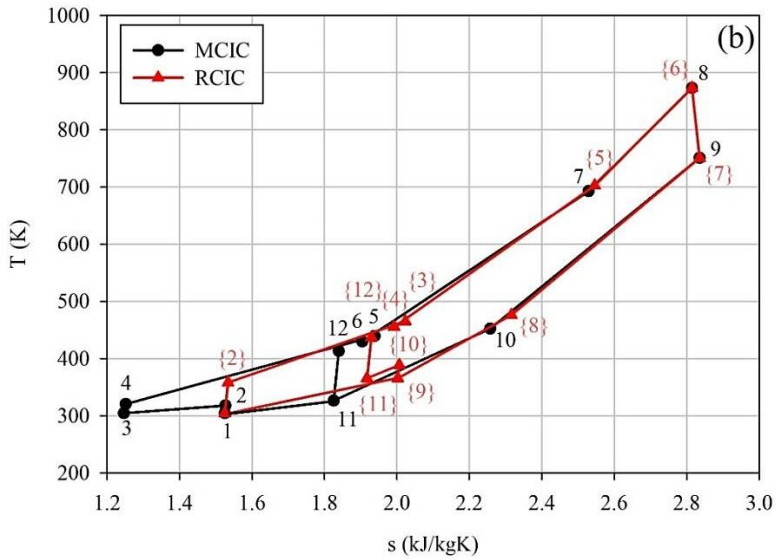

Figure 3. T-s diagram of (a) MCRCIC versus MCIC and (b) RCIC versus MCIC

Effects of SF and RPR$_{RC}$ on Performance Parameters of MCRCIC

In this section, the effects of SF and RPR_{RC} on the MCRCIC performance parameters, especially the thermal efficiency, are focused. The maximum thermal efficiency of MCRCIC at each case of SF and RPR_{RC} is compared with the thermal efficiency of MCIC when other operating parameters are fixed. The operating parameters displayed in Table 3 are employed again, except SF and RPR_{RC}. To find the optimal value of SF and RPR_{RC}, these two parameters are varied and the MCRCIC efficiency is investigated. Moreover, other performance parameters of MCRCIC, i.e. recompression power and heat rejected, are also investigated in this section.

Figure 4 illustrates the thermal efficiency of MCRCIC for $0.35 \le SF \le 0.75$ and $0.0 \le RPR_{RC} \le 0.5$. The maximum efficiency in these ranges of SF and RPR_{RC} is found as 47.580% taking place at $SF = 0.645$ and $RPR_{RC} = 0.0$. It can be implied that at a specific RPR_{MC} the thermal efficiency of MCRCIC is less than that of MCIC because the maximum thermal efficiency of MCRCIC occurs at $RPR_{RC} = 0.0$ at which MCRCIC becomes MCIC. The argumentation issue mentioned at the discussion of Table 3 is responded here.

For MCRCIC cycle, it has the same power generated from the turbine and power required in main compressor as these of MCIC, The recompression with intercooling should be the major effect to the thermal efficiency of the cycle. Operating MCRCIC with low RPR_{RC} value, it indicates that the recompression at the first stage raises small pressure comparing to the required pressure at the recompression outlet state (state (14)). Therefore, the intercooling rejects small amount of heat. Operating cycle with high RPR_{RC} value, it means that the first stage of recompression process raises higher pressure of working fluid. The temperature of working fluid after the first stage recompression is also higher. Passing through the intercooler before flowing to the second stage recompression, the working fluid is rejected more heat rate to have the same temperature as that of inlet state of the first stage recompression. Therefore, more added heat is finally required in the heater as have been mentioned in the above discussion.

For low SF value, it indicates that high portion of working fluid separately flows into recompressor. The intercooling in the recompression process becomes more important for increasing the efficiency by decreasing recompression power in the second stage. Thus, at each SF value, the maximum efficiency at lower SF takes place at higher RPR_{RC}. For example, at $SF = 0.4$, the maximum efficiency is 42.042% occurring at $RPR_{RC} = 0.23$ Comparing with $SF = 0.645$, the maximum efficiency, 47.580%, expresses at $RPR_{RC} = 0.0$. Figure 5 presents that at $SF = 0.645$, when RPR_{RC} increases, the first stage recompression power increases and the second stage recompression power decreases. However, the decreasing rate of the second recompression power is higher than the increasing rate of the first stage recompression power. The total power required in the recompression, then, decreases as RPR_{RC} increases. However, the power saving in the second stage recompression due to using intercooler has less benefit than disadvantage of increasing added heat in the heater. It finally results lower thermal efficiency of MCRCIC, compared to that of MCIC.

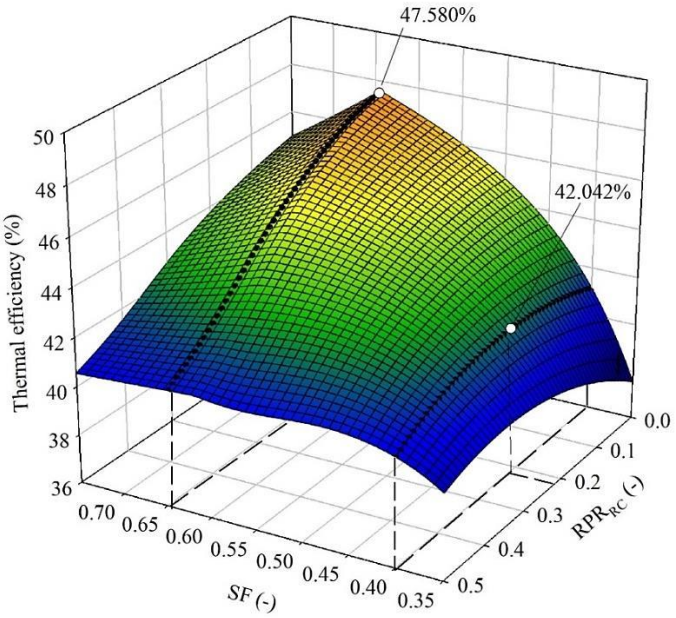

Figure 4. Thermal efficiency of MCRCIC at different SF and RPR_{RC}

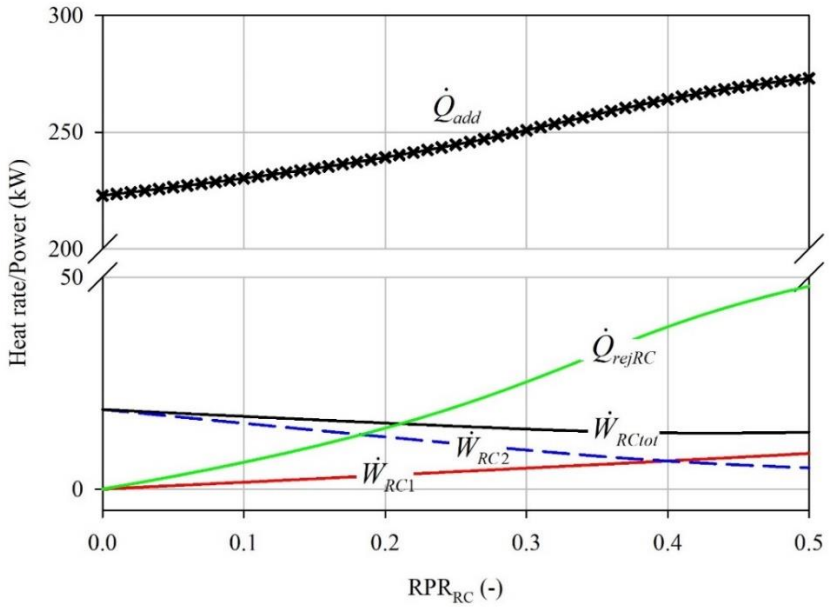

Figure 5. Recompression powers, rejected heat rate and added heat rate of MCRCIC at different RPR_{RC} for $SF = 0.645$

Effects of SF and RPR$_{RC}$ on Performance Parameters of RCIC

The effects of SF and RPR_{RC} on the RCIC performance parameters are observed. The operating parameters shown in Table 3 are used again, except SF and RPR_{RC} the values of SF and RPR_{RC} are varied. The study ranges of SF and RPR_{RC} are $0.35 \le SF \le 0.75$ and $0.0 \le RPR_{RC} \le 0.5$, respectively and the RCIC thermal efficiency is investigated. The study result is shown in Figure 6.

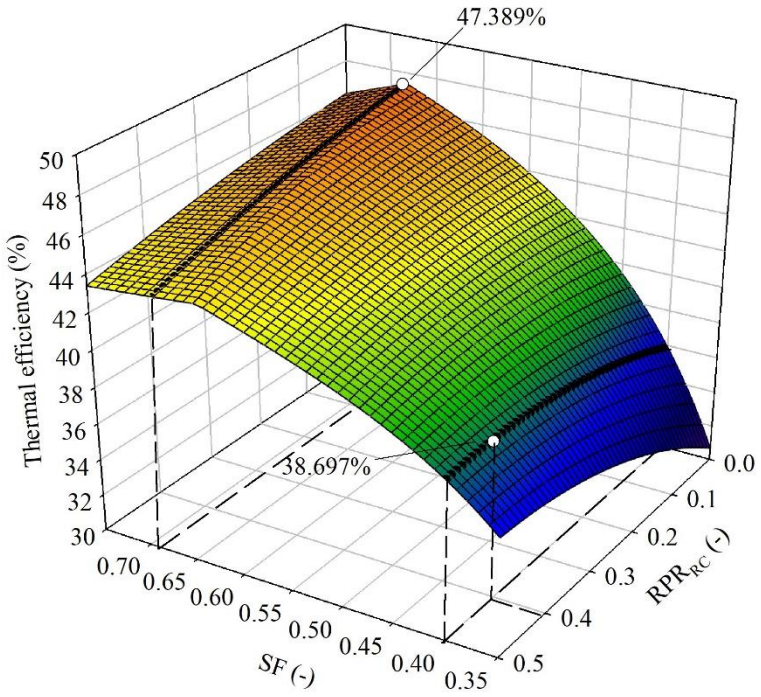

Figure 6. Thermal efficiency of RCIC at different SF and RPR_{RC}

From Figure 6, the maximum thermal efficiency of RCIC is found at $RPR_{RC} = 0.0$ and $SF = 0.682$. RCIC has no intercooler in the main compression. At low SF value, most of working fluid flows through the recompressor. The power consumed in the recompressor is obviously higher than that in the main compressor. Operating cycle with high RPR_{RC} value, the pressure and temperature of working fluid are sharply increased in the first stage recompression. The intercooling can save the power required in the second stage recompression. As found in Figure 6, for low SF value, the thermal efficiency increases with increasing RPR_{RC}. Enlarging RPR_{RC} beyond the optimal value may cause reducing thermal efficiency due to increasing compression power required in the first stage recompression and the intercooling rejects more heat from the cycle. As illustrated in Figure 6, at $SF = 0.4$ the maximum efficiency is 38.697% which occurs at $RPR_{RC} = 0.410$. If RPR_{RC} increases beyond 0.410, the thermal efficiency begins to decline.

For increasing SF, high portion of working fluid flows through the main compressor and the working fluid is rejected heat by the precooler before it is compressed in the main compressor to keep P_1 and T_1 at specific values. The power consumed in the main compressor slightly increases, because the inlet and outlet states of the main compression are fixed. The power required by the recompressor decreases because of increasing SF. The total compression work, then, reduces. It finally results the increase of thermal efficiency.

Figure 7 shows some important performance parameters of RCIC, the recompression powers, rejected heat rate in recompression intercooler, and added heat rate at $SF = 0.682$. The behaviors of these parameters when RPR_{RC} changes show similar as that found in MCRCIC. However, it is observed that the added heat rate in RCIC is generally lower than that in MCRCIC. This is due to the fact that RCIC has no intercooling in the main compression. Even the comparison is done at the same SF, the added heat rate in RCIC is also lower than that in MCRCIC.

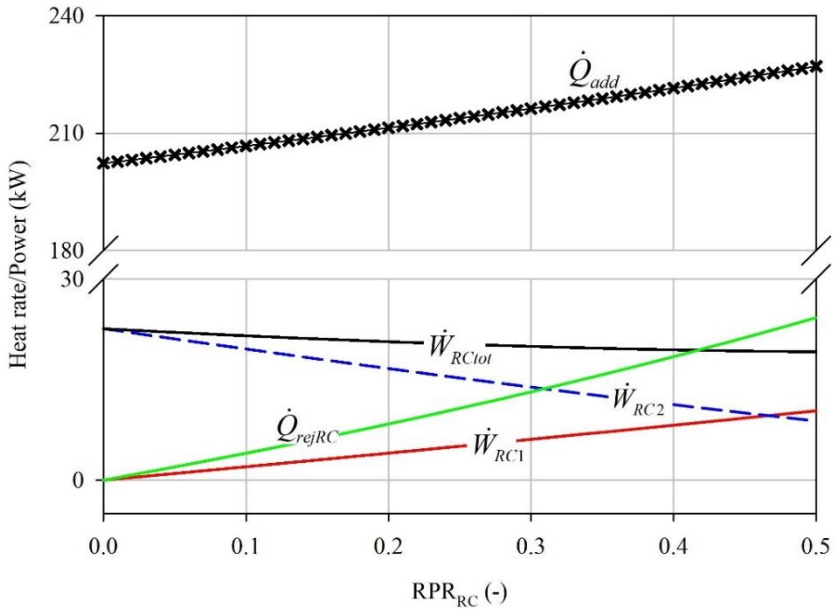

Figure 7. Recompression powers, rejected heat rate and added heat rate of RCIC at different RPR_{RC} for $SF = 0.682$

In general, the effects of SF and RPR_{RC} on the thermal efficiencies of MCRCIC and RCIC are quite similar. Nevertheless, at specific value of SF and RPR_{RC} , MCRCIC and RCIC have different thermal efficiencies. Figure 8 compares the thermal efficiencies of MCRCIC and RCIC in the same ranges of SF and RPR_{RC} . Operating with low RPR_{RC} and low SF values, MCRCIC gives better thermal efficiency, while RCIC provides better thermal efficiency at lower RPR_{RC} and higher SF .

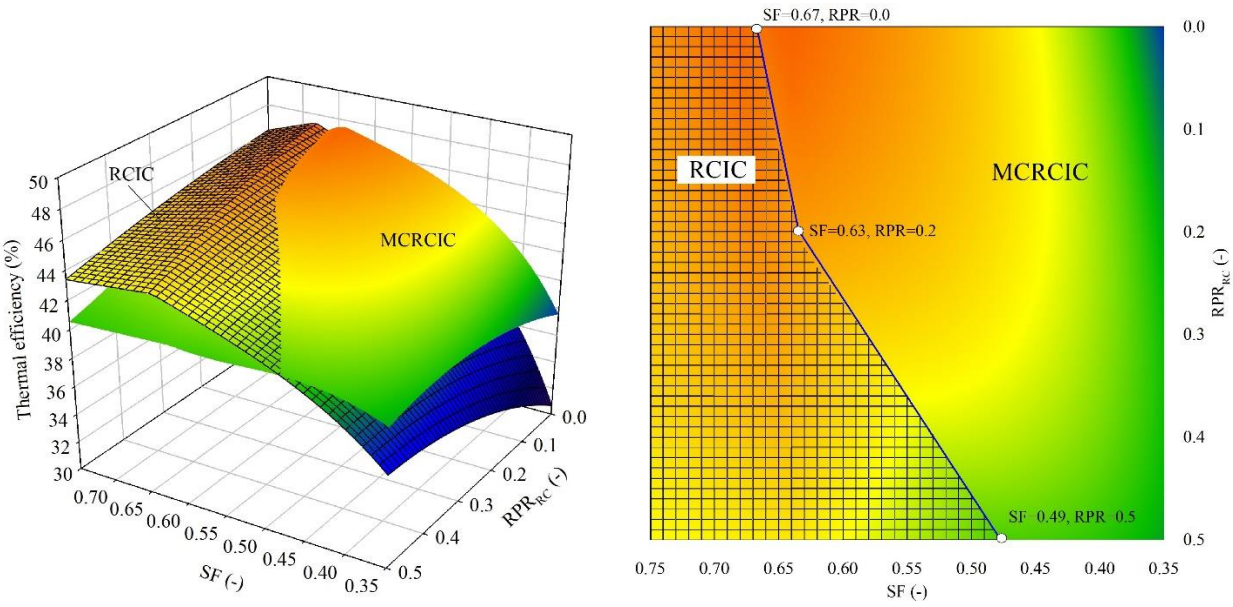

Figure 8. Comparison of thermal efficiency of MCRCIC (without mesh) and RCIC (with mesh) for the same ranges of SF and RPR_{RC}

CONCLUSIONS

The effect of intercoolings applied in the main compression and the recompression processes in the supercritical carbon dioxide recompression Brayton cycle was studied. The first cycle is called MCRCIC in which the intercoolings are applied in the main compression and the recompression processes. The second cycle, called RCIC, has the intercooling in only the recompression process. The thermal efficiencies of both cycles were compared with that of the recompression Brayton cycle with the intercooling in only the main compression or MCIC. The study result indicated that the additional intercooling applied in the recompression process in MCRCIC not only reduces the recompression power but also rejects

heat from the cycle. More heat is, then, required in the heater to raise the working fluid to the maximum cycle temperature. It finally decreases the thermal efficiency and the thermal efficiency of MCRCIC is, therefore, less than that of MCIC. For RCIC in which the intercooling applied in only the recompression, it has lower thermal efficiency than that of MCIC. Based on the simulation result of both cycles, the intercooling applied in the recompression process causes the disadvantage to the thermal efficiency of the cycles. For the effects of RPR_{RC} and SF to the thermal efficiencies of MCRCIC and RCIC, when RPR_{RC} increases, the rejected heat increases and it, consequently, decreases the thermal efficiencies of the cycles. The thermal efficiency of MCRCIC and RCIC increases as SF increases, then, the thermal efficieny decreases when SF is beyond the optimal value.

REFERENCES

[1] Y. Ahn, S.J. Bae, M. Kim, S.K. Cho, S.J. Baik, K.I. Lee, and J.E. Cha, "Review of supercritical CO_2 power cycle technology and current status of research and development," *Nucl. Energy Technol.*, vol. 47, no. 6, pp. 647-661, 2015, doi: 10.1016/j.net.2015.06.009.

[2] R. Span and W. Wagner, "A new equation of state for carbon dioxide covering the fluid region from the triple-point temperature to 1100K at pressures up to 800 MPa," *J. Phys. Chem. Ref. Data*, vol. 25, pp. 1509-1596, 1996, doi:10.1063/1.555991.

[3] F. Crespi, G. Gavagnin, D. Sánchez, and G.S. Martínez, "Supercritical carbon dioxide cycles for power generation: a review," *Appl. Energy*, vol. 195, pp.152-158, 2017, doi: 10.1016/j.apenergy.2017.02.048.

[4] M.T. Luu, D. Milani, R. McNaughton, and A. Abbas, "Analysis for flexible operation of supercritical CO_2 Brayton cycle integrated with solar thermal systems," *Energy*, vol. 124, pp. 752-771, 2017, doi: 10.1016/j.energy.2017.02.040.

[5] V.T. Cheang, R.A. Hedderwick, and C. McGregor, "Benchmarking supercritical carbon dioxide cycles against steam Rankine cycles for concentrated solar power," *Sol. Energy*, vol. 113, pp. 199-211, 2015, doi: 0.1016/j.solener.2014.12.016.

[6] F.A. Al-Sulaiman and M. Atif, "Performance comparison of different supercritical carbon dioxide Brayton cycles integrated with a solar power tower," *Energy*, vol. 82, pp. 61-71, 2015, doi: 10.1016/j.energy.2014.12.070.

[7] D.V. Di Maio, A. Boccitto, and G. Caruso, "Supercritical carbon dioxide applications for energy conversion systems," *Energy Proc.*, vol. 82, pp. 819-824, 2015, doi: 10.1016/j.egypro.2015.11.818.

[8] J.J. Dyreby, *Modeling the Supercritical Carbon Dioxide Brayton Cycle with Recompression*, PhD thesis, University of Wisconsin-Madison, 2014.

[9] D. Novales, A. Erkoreka, V. De la Peña, and B. Herrazti, "Sensitivity analysis of supercritical CO2 power cycle energy and exergy efficiencies regarding cycle component efficiencies for concentrating solar power," *Energy Convers. Manage.*, vol. 182, pp. 430-450, 2019, doi: 10.1016/j.enconman.2018.12.016.

[10] M. Saeed, S. Khatoon, and M.H. Kim, "Design optimization and performance analysis of a supercritical carbon dioxide recompression Brayton cycle based on the detailed models of the cycle components," *Energy Convers. Manage.*, vol. 196, pp. 242-260, 2019, doi: 10.1016/j.enconman.2019.05.110.

[11] M.A. Reyes-Belmonte, A. Sebastián, M. Romero, and J. González-Aguilar, "Optimization of a recompression supercritical carbon dioxide cycle for an innovative central receiver solar power plant," *Energy*, vol. 112, pp. 17-27, 2016, doi: 10.1016/j.energy.2016.06.013.

[12] K. Wang and Y.L. He, "Thermodynamic analysis and optimization of a molten salt solar power tower integrated with a recompression supercritical CO_2 Brayton cycle based on integrated modeling," *Energy Convers. Manage*., vol. 135, pp. 336-350, 2017, doi: 10.1016/j.enconman.2016.12.085.

[13] J. Sarkar and S. Bhattacharyya, "Optimization of recompression S-CO_2 power cycle with reheating," *Energy Convers. Manage.*, vol. 50, no. 8, pp. 1939-1945, 2009, doi: 10.1016/j.enconman.2009.04.015.

[14] Y. Ma, M. Liu, J. Yan, and J. Lui, "Thermodynamic study of main compression intercooling effects on supercritical CO_2 recompression Brayton cycle," *Energy*, vol. 140, pp. 746-756, 2017, doi: 10.1016/j.energy.2017.08.027.

[15] E. Ruiz-Casanova, C. Rubio-Maya, J.J. Pacheco-Ibarra, V.M. Ambriz-Díaz, C.E. Romero, and X. Wang, "Thermodynamic analysis and optimization of supercritical carbon dioxide Brayton cycles for use with low-grade geothermal heat sources," *Energy Convers. Manage.*, vol. 216, pp. 112978, 2020, doi: 10.1016/j.enconman.2020.112978.

[16] J. Yang, Z. Yang, and Y. Duan, "Part-load performance analysis and comparison of supercritical CO_2 Brayton cycles," *Energy Convers. Manage.*, vol. 214, pp. 112832, 2020, doi: 10.1016/j.enconman.2020.112832.

[17] K. Wang, Y.L. He, and H.H. Zhu, "Integration between supercritical CO_2 Brayton cycles and molten salt solar power towers: a review and a comprehensive comparison of different cycle layouts," *Appl. Energy*, vol. 195, pp. 819-836, 2017, doi: 10.1016/j.apenergy.2017.03.099.

[18] X. Wang, Q. Liu, J. Lei, W. Han, and H. Jin, "Investigation of thermodynamic performances for two-stage recompression supercritical CO2 Brayton cycle with high temperature thermal energy storage system," *Energy Convers. Manage.*, vol. 165, pp. 477-487, 2018, doi: 10.1016/j.enconman.2018.03.068.

[19] Z. Rao, T. Xue, K. Huang, and S. Liao, "Multi-objective optimization of supercritical carbon dioxide recompression Brayton cycle considering printed circuit recuperator design," *Energy Convers. Manage.*, vol. 201, pp. 112094, 2019, doi: 10.1016/j.enconman.2019.112094.

[20] N.D. Baltadjiev, C. Lettieri, and Z.S. Spakovszky, "An investigation of real gas effects in supercritical CO2 centrifugal compressors," *J. Turbomach.*, vol. 137, no. 9, pp. 091003, 2015, doi: 10.1115/1.4029616.

[21] B. Halimi and K.Y. Suh, "Computational analysis of supercritical CO2 Brayton cycle power conversion system for fusion reactor," *Energy Convers. Manage.*, vol. 63, pp. 38-43, 2012, doi: 10.1016/j.enconman.2012.01.028.

[22] Thermophysical Properties of Fluid Systems, National Institute of Standards and Technology, 2018. [Online]. Available: https://webbook.nist.gov/chemistry/fluid/

[23] A. Moisseytsev and J.J. Sienicki, *Development of a Plant Dynamics Computer Code for Analysis of a Supercritical Carbon Dioxide Brayton Cycle Energy Converter Coupled to a Natural Circulation Lead-Cooled Fast Reactor*, Report, US: Argonne National Laboratory, 2006.